Article

Not peer-reviewed version

The Therapeutic Potential of Adipose-Derived Mesenchymal Stem Cell Secretome in Osteoarthritis: A Comprehensive Study

Elsa González-Cubero , María Luisa González-Fernández , Marta Esteban Blanco , Saúl Pérez-Castrillo , Esther Pérez-Fernández , Nicolás Navasa , Ana M Aransay , Juan Anguita , Vega Villar-Suárez *

Posted Date: 19 September 2024

doi: 10.20944/preprints202409.1449.v1

Keywords: Mesenchymal stem cells; osteoarthritis; conditioned medium; secretome; inflammatory cytokines

Article

The Therapeutic Potential of Adipose-Derived Mesenchymal Stem Cell Secretome in Osteoarthritis: A Comprehensive Study

Elsa González-Cubero [1,2], Maria Luisa González-Fernández [2], Marta Esteban-Blanco [2], Saúl Pérez-Castrillo [2], Esther Pérez-Fernández [2], Nicolás Navasa [3,4], Ana M. Aransay [4,5], Juan Anguita [4,6] and Vega Villar-Suárez [2,7,*]

1 Department of Neurosurgery, Stanford School of Medicine, Stanford University, Palo Alto, California, USA
2 Department of Anatomy, Faculty of Veterinary Sciences, Campus de Vegazana, University of Léon-Universidad de León, 24071 Spain
3 Department of Molecular Biology, Faculty of Veterinary Sciences, Campus de Vegazana, University of Léon-Universidad de León, 24071 Spain
4 Center for Cooperative Research in Biosciences (CIC bioGUNE)-Basque Research and Technology Alliance (BRTA), Parque Tecnológico de Bizkaia, Building 801-A, 48160, Derio, Bizkaia, Spain
5 CIBERehd, ISCIII, Madrid, Spain
6 IKERBASQUE, Basque Foundation for Science, Bilbao, Spain
7 Institute of Biomedicine (IBIOMED), Faculty of Veterinary Sciences, Campus de Vegazana, University of León-Universidad de León 24071, Spain
* Correspondence: vega.villar@unileon.es

Abstract: Osteoarthritis (OA) is a degenerative joint disease characterized by cartilage degradation and inflammation. This study investigates the therapeutic potential of secretome derived from adipose tissue mesenchymal stem cells (ASCs) in mitigating inflammation and promoting cartilage repair in an *in vitro* model of OA. Our *in vitro* model comprised chondrocytes inflamed with TNF. To assess the therapeutic potential of secretome, inflamed chondrocytes were treated with it and concentrations of pro-inflammatory cytokines, metalloproteinases (MMPs) and extracellular matrix markers were measured. In addition, secretome-treated chondrocytes were subject to a microarray analysis to determine which genes were upregulated and which were downregulated. Treating TNF-inflamed chondrocytes with secretome *in vitro* inhibits the NF-κB pathway, thereby mediating anti-inflammatory and anti-catabolic effects. Additional protective effects of secretome on cartilage are revealed in the inhibition of hypertrophy markers such as RUNX2, COLX and increases in Col2a1 and ACAN production as well as the upregulation of Sox-9. These findings suggest that ASC-derived secretome can effectively reduce inflammation, promote cartilage repair, and maintain chondrocyte phenotype. This study highlights the potential of ASC-derived secretome as a novel, non-cell-based therapeutic approach for OA, offering a promising alternative to current treatments by targeting inflammation and cartilage repair mechanisms.

Keywords: mesenchymal stem cells; osteoarthritis; conditioned medium; secretome; inflammatory cytokines

1. Introduction

Osteoarthritis (OA) is one of the most common diseases of the joints and their surrounding tissues and was recorded as the fourth major cause of disability in 2020 [1]. OA attacks cartilage, causing it to deteriorate. It also leads to alterations in the subchondral bone and synovium, as well as producing underlying bone damage and morphological changes such as subchondral sclerosis, subchondral bone cysts, osteophyte formation, and synovitis [2]. The tissue most affected by OA is hyaline cartilage; the disease alters cell-matrix interactions slowly destroying tissue integrity [3].

 doi:10.20944/preprints202409.1449.v

Although many aspects of OA pathogenesis are still not fully understood, it is thought that the persistent synthesis of several mediators by articular tissues contributes to tissue deterioration. Inflammation is currently thought to play an important role in the early phases of OA development as well as in its progression [3,4]. Experimentally it has been shown that the release of certain inflammatory substances such pro-inflammatory cytokines is one of the main mediators of altered metabolism and increased cartilage catabolism in OA [5]. The activity of cytokines on articular chondrocytes is of significant interest in the study of OA as these signaling molecules are proven to cause cartilage breakdown by upregulating inflammatory or catabolic genes and downregulating anti-inflammatory or anabolic genes [6]. In particular, TNF and IL-1, have been shown to alter the expression of various factors in ways that tend to increase the catabolic activity of chondrocytes, causing cartilage matrix degradation, for example, by reducing levels of aggrecan (ACAN) or type II collagen (Col2a1) [6] and by increasing the production of matrix metalloproteinases (MMPs) [7,8], prostaglandin E2 (PGE2) [9], cytokines, chemokines, reactive oxygen species, and nitric oxide (NO) [4,9,10]. Chondrocytes may revert to a developmental molecular program if these pathways are disrupted, resulting in the production of chondrocyte hypertrophy markers such as COLX, MMP-13, and RUNX2 [11].

Currently there is a wide range of therapies for inflammatory pathologies such as OA. Unfortunately, many of these treatments are expensive, nonspecific, and none of them can offer drug-free pain relief. In the last decade, however, novel therapies based on mesenchymal stem or stromal cells (MSCs) have emerged as promising candidates to treat OA [12,13] and certain other musculoskeletal problems [14].

Initially, it was thought that the therapeutic effects of transplanted MSCs were a result of MSCs migrating to the damaged region and differentiating to replace dead or damaged cells. However, recent research suggests that benefits of MSCs are achieved due to their secretion of trophic factors [15]. These factors are present in MSC secretome, also known as conditioned medium (CM). It contains the paracrine soluble substances and extracellular vesicles (EVs) and these proteins are thought to be responsible of angiogenesis regulation, immunological response, tissue protection, and wound healing. As a result, there could be significant therapeutic benefits from substituting MSCs for the trophic factors found in MSC secretome [16,17].

This study aims to assess the protective effects of secretome from adipose tissue derived-MSCs (ASCs) against inflammation in an *in vitro* pro-inflammatory model. We examine the impact of secretome on cytokines and factors responsible for inflammation and tissue degeneration in OA.

2. Results

2.1. ASC-Derived Secretome Downregulates the Expression of iNOS, IL-6, MMP-13, and TNF

Initially it was necessary to determine whether ASC-derived secretome had any ability to modulate the expression of certain key mediators of inflammation (iNOS, IL-6, MMP-13 and TNF). To this end, qPCR was used to observe the expression of these mediators in our four sample types: non-inflamed chondrocytes, ASCs, TNF-inflamed chondrocytes, and CM-treated TNF-inflamed chondrocytes. Figure 1 shows firstly significant increases in IL-6 and MMP-13 expression for TNF-inflamed chondrocytes compared to non-inflamed chondrocytes and secondly that the treatment of chondrocytes with secretome dramatically reduced the expression of these mediators.

Regarding TNF and iNOS, a similar pattern was observed, i.e., the expression of these mediators increased in response to TNF exposure and decreased in the presence of secretome.

 doi:10.20944/preprints202409.1449.v

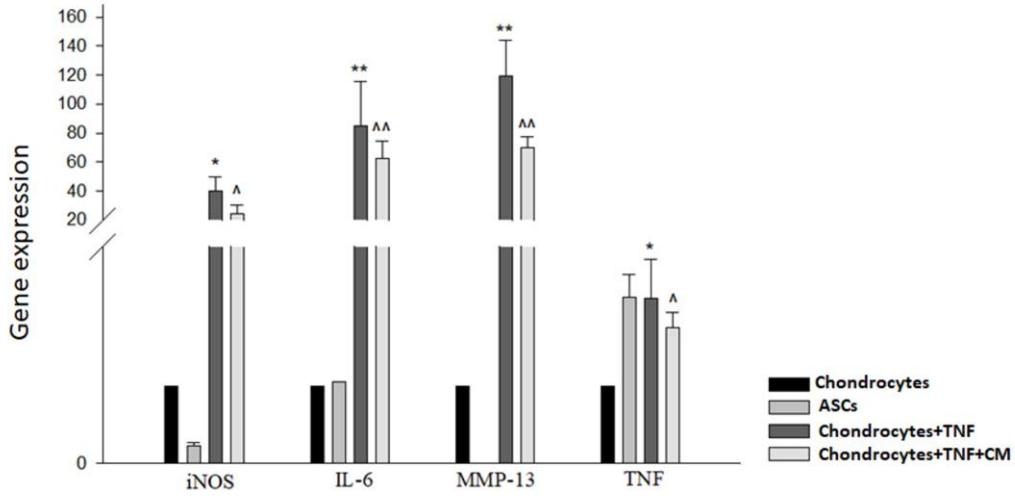

Figure 1. TNF-induced modulation of inflammatory cytokines with and without CM treatment. qPCR was used to measure the relative gene expression of iNOS, IL-6, MMP-13 and TNF genes in non-inflamed chondrocytes, ASCs, TNF-inflamed chondrocytes and CM-treated TNF-inflamed chondrocytes after 12 h of incubation. The results are expressed as the mean ± SD of three independent experiments. * ($p \leq 0.05$), ** ($p \leq 0.01$) compared to non-stimulated cells ^ ($p \leq 0.05$), ^^ ($p \leq 0.01$) compared to TNF-stimulated cells.

2.2. ASC-Derived Secretome Induces Downregulation of Catabolic Markers and Upregulation of Anabolic Markers

Based on the results obtained by qPCR, further investigation was required to identify the specific genes that might be activated by secretome to give the anti-inflammatory response observed. To this end, a DNA microarray was performed to compare changes in gene expression between two sets of experimental samples: a) TNF inflamed chondrocytes and non-inflamed chondrocytes (Cond TNF comparison/control condition) and b) TNF inflamed chondrocytes and CM-treated and TNF-inflamed chondrocytes (Cond TNF-CM treated comparison/Cond TNF).

Beginning with the TNF-inflamed/non-inflamed chondrocyte comparison, screening identified a total of 539 DEGs including 412 positively regulated genes and 128 negatively regulated genes. The analysis was repeated to compare gene expression in the Condrocytes TNF-CM treated comparison/Condrocytes TNF. Here, screening identified a total of 91 DEGs, including 46 positively regulated genes and 45 negatively regulated genes. DEG functional annotation analysis for these two groups of cells is shown on Figure 2A and 2B and can be summarized as follows: altered genes were mainly involved in (i) molecular functions related to catalytic activity; (ii) the synthesis of cellular components such as organelles, membranes, and families of hydrolytic enzymes, ligases, proteases, among others; (iii) cellular processes such as cell communication.

 doi:10.20944/preprints202409.1449.v

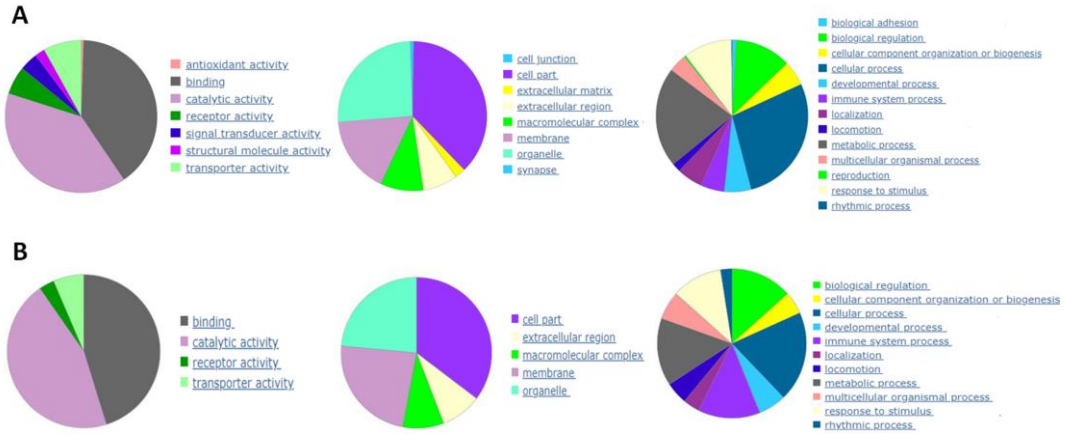

Figure 2. Functional annotation analysis of DEGs that were significantly downregulated or upregulated (A) comparing gene expression in non-inflamed chondrocytes and TNF-stimulated chondrocytes and (B) comparing gene expression in TNF-inflamed chondrocytes and CM-treated TNF-inflamed chondrocytes.

Table 1 shows a summary of the top genes that were significantly differently regulated involved in either anabolism or catabolism in our in vitro model of OA. Within the TNF-inflamed chondrocyte comparison with control condition group, the gene most positively upregulated were those encoding for CCL5 (chemokine ligand 5), also called RANTES (+270.88-fold) and CCL2 (chemokine ligand 2), known as monocyte chemoattractant protein-1 (MCP-1) (+131.97-fold) they act as a chemoattractant for immune cells, particularly monocytes and T cells. They play a role in recruiting inflammatory cells to the joint and promoting chronic inflammation in OA [23]. It is clear that genes involved in catabolism such as MMPs [24] [MMP3 (+161.50-fold) and MMP1 (+115.76-fold)], ADAMTS (+ 13.39-fold) and pro-inflammatory cytokines such as IL6 (+136.82-fold) are all upregulated in the TNF-inflamed/non-inflamed chondrocyte comparison while, in contrast, they are downregulated in the CM-treated-TNF-inflamed chondrocyte/TNF-inflamed comparison. Furthermore, for genes involved in anabolism such as ACAN (+10.61-fold), Col2a1 (+10.01-fold), TIMPs [TIMP2 (-10.20-fold) and TIMP4 (-10.07-fold)] and Versican (+10.07-fold), the opposite trend is seen: these genes were downregulated in the TNF-inflamed/ non-inflamed chondrocyte comparison and upregulated in the CM-treated-TNF-inflamed /TNF-inflamed chondrocyte comparison. This highlight, once again, the immunomodulatory potential of ASC-derived secretome.

 doi:10.20944/preprints202409.1449.v

Table 1. Genes differentially expressed between TNF inflamed-chondrocytes and control and chondrocytes-TNF inflamed with CM and chondrocytes-TNF inflamed.

CATABOLISM			ANABOLISM		
Type of compound	**Up-regulated Cond TNF/ctrl**	**Down-regulated Cond TNF MC/Cond TNF**	**Type of compound**	**Down-regulated Cond TNF/ctrl**	**Up-regulated Cond TNF MC/Cond TNF**
Factor Nuclear Kappa B	NFKBIA (31.84) NFKB2 (18.05) NFKB1 (16.39) NFKBIZ (16.17)	NFKBIA (-12.609) NFKB2 (-10.74) NFKB1 (-10.58) NFKBIZ (-14.00)	Cartilage extracellular matrix proteins	Col2A1 (-10.02) ACAN (-10.63) VCAN (-15.29)	Col2A1 (10.01) ACAN (10.61) VCAN (10.079)
Interleukins	IL1RN (14.38) IL15RA (19.74) IL15 (15.29) IL4I1 (33.98) IL17RB (22.36) IL6 (136.82) LIF (21.39)	IL1RN (-11.77) IL15RA (-12.52) IL15 (-11.52) IL4I1 (-10.48) IL17RB (-14.33) IL6 (-11.70) LIF (-12.39)	Insulin-like growth factors	IGF2R (-10.82) IGFBP6 (-10.95) IGFBP2 (-10.30) IGF2BP2 (-11.52) IGFBP1 (-11.89)	IGF2R (10.05) IGFBP6 (12.20) IGFBP2 (10.11) IGF2BP2 (11.51) IGFBP1 (10.50)
Chemokines	CCL5 (270.88) CCL2 (113.97) CCL20 (62.16)	CCL5 (-17.506) CCL2 (-12.58) CCL20 (-11.84)	Fibroblast growth factors	FGF23 (-10.26) FGFRL1 (-15.04)	FGF23 (10.01) FGFRL1 (1.01)
Metalloproteinases	MMP13 (39.81) MMP1 (115.76) MMP3 (161.50)	MMP13 (-13.78) MMP1 (-1.27) MMP3 (1.73)	Transforming growth factor Beta	TGFB1I1 (-11.13)	TGFB1I1 (1.13)
A desintegrin and metalloproteinase with thrombospondin motifs	ADAMTS5 (13.39) ADAMTS9 (13.28) ADAMTS1 (12.21) ADAMTS13 (10.96) ADAMTS7 (10.04)	ADAMTS5 (-10.40) ADAMTS9 (-11.041) ADAMTS1 (-10.68) ADAMTS13 (-10.32) ADAMTS7 (-10.56)	Platelet-derived growth factors	PDGFA (-10.56) PDGFB (-10.29) PDGFC (-12.19) P DGFD (-10.59)	PDGFA (10.24) PDGFB (10.38) PDGFC (10.54) PDGFD (10.36)
Tumor necrosis factor	TNFSF13B (77.57) C1QTNF1 (71.40) TNFAIP6 (65.74) TNFAIP3 (49.17) TNFAIP2 (21.79)	TNFSF13B (-15.59) C1QTNF1 (-12.40) TNFAIP6 (-14.03) TNFAIP3 (-11.42) TNFAIP2 (-13.16)	Multiple EGF Like Domains 10	MEGF10 (-10.66)	MEGF10 (10.27)
			Vascular Endothelial Growth Factor	VEGFB (-1.12)	VEGFB (10.71)
			Bone morphogenetic protein receptor	BMPR1A (-10.03)	BMPR1A (10.21)
			Interleukin 13	IL13RA1 (-10.92)	IL13RA1 (10.14)
			Metallopeptidase inhibitor	TIMP2 (-10.20) TIMP4 (-10.07)	TIMP2 (10.40) TIMP4 (10.59)
			Mothers against decapentaplegic homolog	SMAD2 (-10.67) SMAD5 (-11.77)	SMAD2 (10.36) SMAD5 (1.045)

1

2.3. ASC-Derived Secretome Mitigates TNF-Induced MMP and ADAMTS-5 Activity

MMPs and ADAMTS-5 are known to have a role in cartilage degeneration and the development of OA [25]. Thus, we assessed the levels of these molecules in cell supernatants to observe the therapeutic effects of secretome on inflamed chondrocytes. In this way, ELISA was used to examine the production of MMPs (MMP-1, MMP-2, and MMP-13) and ADAMTS-5 in our different experimental conditions (see materials and methods section 3). Results are shown in Figure 3. Chondrocytes express endogenous MMPs in basal conditions and inflammation with TNF increased the production of ADAMTS-5 and all MMPs tested, with the greatest increase being seen for MMP-13. Treatment with secretome reduced the production of MMP-1, MMP-13 and ADAMTS-5 to levels beneath those found in TNF-inflamed chondrocytes with the level of reduction being most

 doi:10.20944/preprints202409.1449.v

pronounced in the case of MMP-13. MMP-2 levels remained very similar under all experimental conditions.

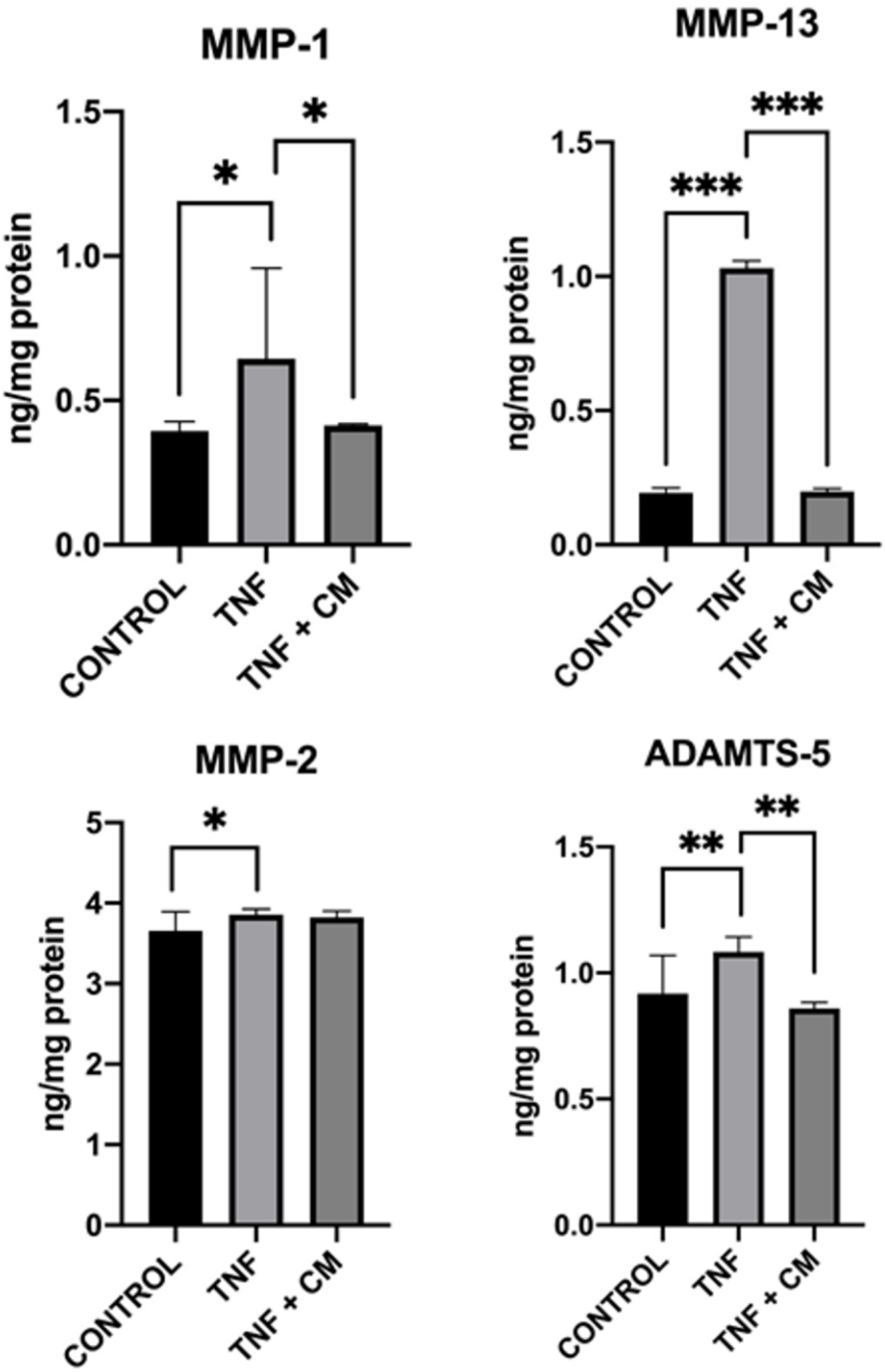

Figure 3. Modulation of MMP-1, MMP-2, MMP-13, and ADAMTS-5 proteins in chondrocytes. ELISA was used to measure protein levels comparing non-inflamed, TNF-inflamed, and CM-treated TNF-inflamed chondrocytes after 12 h of incubation. The results are expressed as the mean ± SD of three independent experiments. p≤*0.05, **p≤0.01, ***p≤ 0..001.

2.4. ASC-Derived Secretome Significantly Reduces Levels of Hypertrophy Markers in Inflamed Chondrocytes

Evidence suggests that the activation of hypertrophic differentiation in articular chondrocytes is a key mechanism in the development of osteoarthritis (OA) [26]. To investigate this process, we analyzed two important markers of hypertrophy: COLX and RUNX2. We conducted three tests to

 doi:10.20944/preprints202409.1449.v

assess how their expression in chondrocytes changes with TNF-α-induced inflammation and how treatment with secretome might mitigate these changes. These tests included qPCR with bone as a positive control (Figure 4A), western blot with β-Actin as an endogenous control (Figure 4B), and immunocytochemical analysis (Figures 4C and D). Consistently across all analyses, we observed upregulation of COLX and RUNX2 in TNF-α-inflamed chondrocytes and downregulation of these markers in conditioned medium (CM)-treated TNF-α-inflamed chondrocytes.

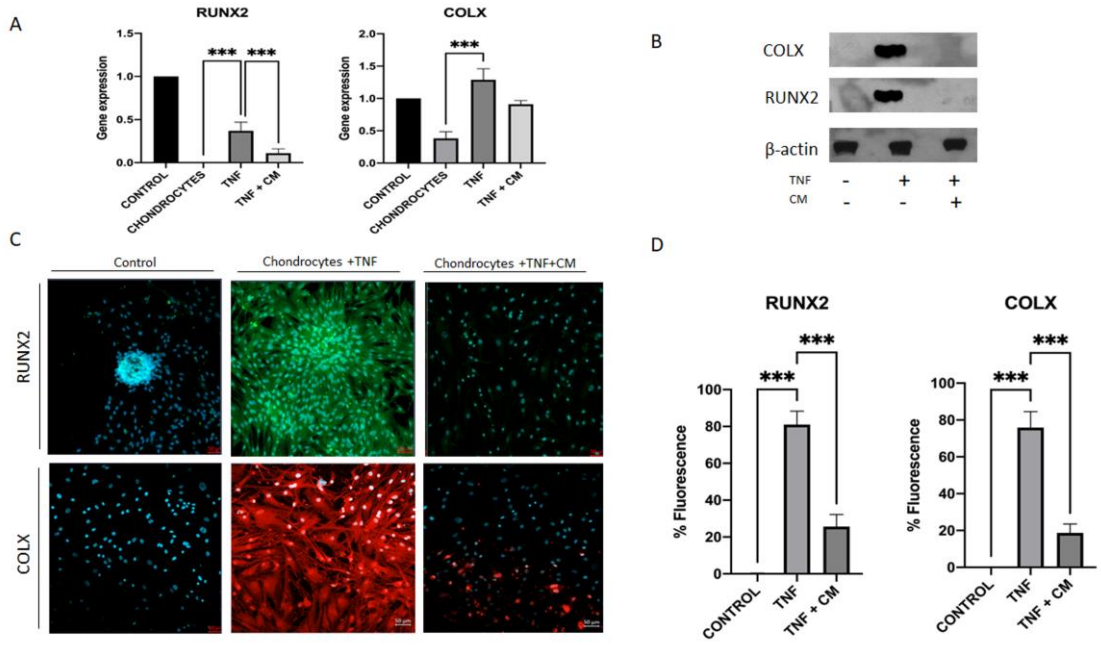

Figure 4. Inflammation-induced upregulation of hypertrophic factors in chondrocytes. RUNX2 and COLX gene expression was determined for non-inflamed, TNF-inflamed, and CM-treated TNF-inflamed chondrocytes after 12h of incubation A) qPCR analysis with bone as control. The results are expressed as the mean ± SD of three independent experiments. ***p≤ 0.001. B) Western blot analysis with β-Actin used as endogenous control. Levels of COLX and RUNX2 were detected only in TNF-inflamed chondrocytes not treated with CM. C) Immunocytochemical analysis (representative image): Blue fluorescence indicates cell nuclei (DAPI); green immunofluorescence shows presence of RUNX2 (Alexa-488); and red immunofluorescence indicates the presence of COLX (Alexa-568). Scale bar: 20-50μm. D) Histogram of RUNX2 and COLX immunofluorescence. The results are expressed as the mean ± SD of three independent experiments. ***p≤ 0.001.

2.5. ASC-Derived Secretome Increases the Expression of Sox-9, Col2a1 and ACAN in TNF-Inflamed Chondrocytes

The expression of specific chondrogenic genes, such as Sox-9, ACAN and Col2a1, was analyzed under all experimental conditions. Analysis using qPCR (Figure 5A) shows that compared to TNF-inflamed chondrocytes, CM-treated TNF-inflamed chondrocytes had increased levels of Col2a1 and ACAN. TNF-inflamed-chondrocytes showed reduced the expression of Col2a1 and ACAN, compared to non-inflamed chondrocytes while for CM-treated TNF-inflamed chondrocytes, levels of these genes returned to near normal (non-inflamed) levels. The expression of Sox-9 in TNF-inflamed chondrocyte samples did not change significantly compared to non-inflamed samples, however, for CM-treated TNF-inflamed chondrocytes the levels far exceeded those seen in non-inflamed samples. In the western blot analysis (Figure 5B), both inflamed chondrocytes and chondrocytes treated with CM exhibited positive bands for Col2a1 and Sox-9. These results indicate the presence of these important markers associated with chondrogenesis and cartilage formation. It is worth noting that in the case of inflamed chondrocytes, the presence of positive bands for Col2a1 and Sox-9 in the western blot was unexpected. Immunocytochemical analysis (Figure 5C-D) showed significant decreases in Col2a1, ACAN and Sox-9 expression for TNF-inflamed chondrocytes compared to non-inflamed

 doi:10.20944/preprints202409.1449.v

samples. For CM-treated TNF-inflamed chondrocytes, however, expression of these three genes was increased compared to levels seen for TNF-inflamed chondrocytes, although the observed increase was significant only for Sox-9.

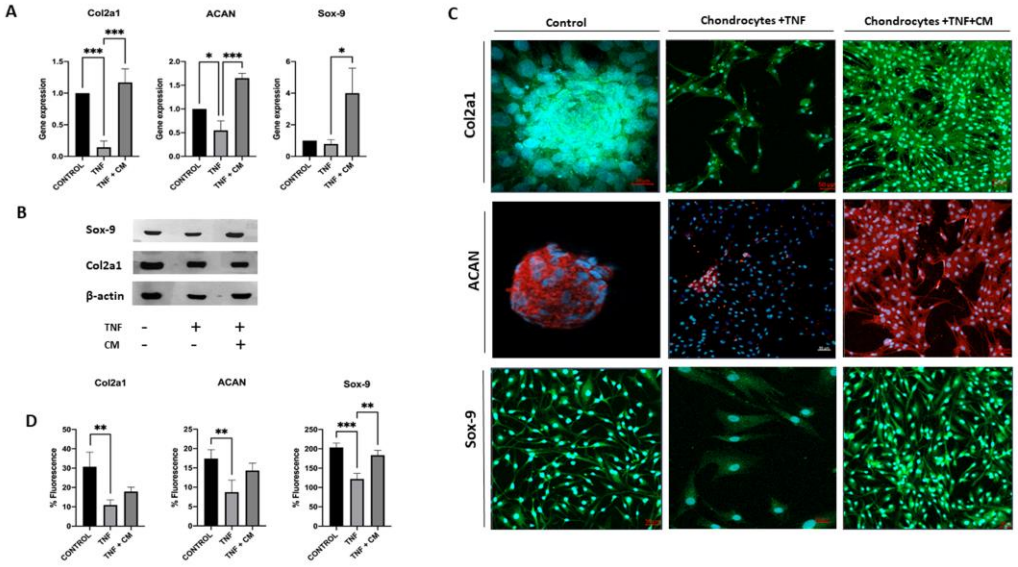

Figure 5. Secretome induced regeneration in inflamed chondrocytes. Gene expression for a range of chondrogenic genes was compared for non-inflamed, TNF-inflamed, and CM-treated TNF-inflamed chondrocytes after 12h of incubation A) qPCR analysis of Col2a1, ACAN and Sox-9. The results are expressed as the mean ± SD of three independent experiments. p≤*0.05, **p≤0.01, ***p≤ 0.001. B) Western blot analysis of Sox-9 and Col2a1; β-Actin was used as endogenous control. C) Immunohistochemical analysis of Col2a1, ACAN and Sox-9 (representative image). Blue fluorescence indicates cell nuclei (DAPI); green immunofluorescence shows presence of Col2a1 (Alexa-488); red immunofluorescence indicates the presence of ACAN (Alexa-568); and green immunofluorescence shows presence of Sox-9 (Alexa-488) D) Histogram showing results for Col2a1, ACAN and Sox-9 immunofluorescence. The results are expressed as the mean ± SD of three independent experiments. **p≤0.01, ***p≤ 0.001.

2.6. ASC-Derived Secretome Increases Chondrocyte Proliferation

Figure 6A-B are fluorescence images showing the influence of TNF and CM-treated TNF-inflamed chondrocytes on chondrocyte proliferation. Comparing cell proliferation rates for non-inflamed chondrocytes, TNF-inflamed, and CM-treated TNF-inflamed chondrocytes (Figure 6B), it is clear that proliferation rates were highest for the CM-treated TNF-inflamed chondrocytes. Furthermore, the inflammatory agent (TNF) appeared to slightly reduce chondrocyte viability, however, the presence of CM stabilized cell viability.

2.7. ASC-Derived CM Inhibits NF-κB Translocation

NF-κB is a well-known transcription factor involved in TNF-induced effects on a variety of inflammatory and catabolic mediators. TNF triggers NF-κB translocation into the nucleus and DNA binding, which in turn induces gene transcription thus, we studied the possible regulation of NF-κB translocation by CM. Figure 6C shows a comparison of TNF-induced p65-NF-κB DNA binding in TNF-inflamed chondrocytes and non-inflamed chondrocytes and clearly demonstrates that TNF inflammation increases p65-NFκB DNA binding. Considering Figure 6C-D together, it is possible to see in detail how ASC-derived CM reduces the TNF-induced elevation in P65-NFκB expression and how CM does in fact appear to block NF-κB translocation.

 doi:10.20944/preprints202409.1449.v

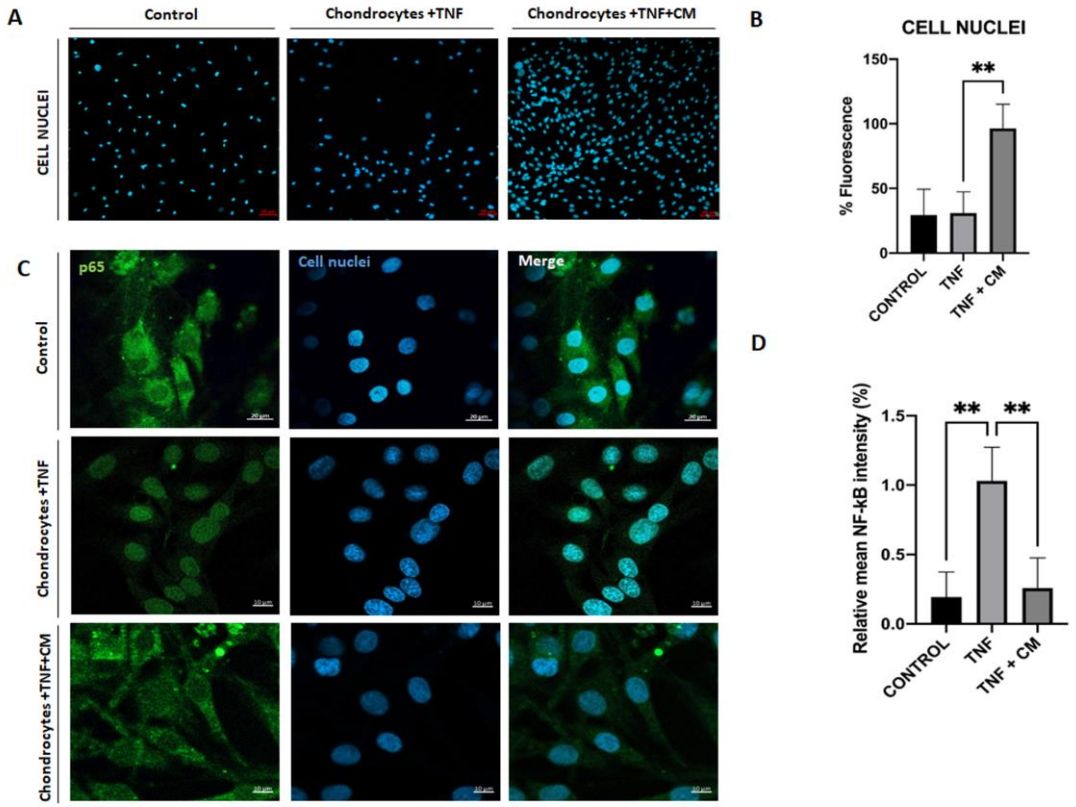

Figure 6. Secretome induced proliferation and blocked NF-κB translocation in inflamed chondrocytes. Non-inflamed, TNF-inflamed, and CM-treated TNF-inflamed chondrocytes were compared after 12h of incubation to assess cell proliferation and NF-κB activation in the various experimental conditions. A) Cell proliferation (representative images). Blue fluorescence indicates cell nuclei (DAPI). Scale bar: 50μm. B) Cell proliferation fluorescence histograms. The results are expressed as the mean ± SD of three independent experiments. **p≤0.01 . C) NF-κB activation (representative image): Blue fluorescence indicates cell nuclei (DAPI) and green immunofluorescence indicates the presence of NF-κB p65 antibodies so enabling the localization of NF-κB p65. Scale bar: 10 μm. D) Relative intensity of green fluorescence observed cell nuclei. The results are expressed as the mean ± SD of three independent experiments. **p≤0.01 ANOVA was used comparing TNF treated samples with all other groups.

3. Discussion

This work provides an in-depth study of the therapeutic effects of secretome or CM on TNF-inflamed chondrocytes and supports the thesis that MSC-derived secretome represents an attractive replacement for traditional regenerative therapies. Secretome contains bioactive compounds with proven paracrine effects and immunomodulatory properties, thus secretome has been proposed as a novel free-cell treatment for OA [27]. Of particular interest in this regard, is the way in which secretome appears to be able to regulate pro-inflammatory and catabolic factors in chondrocytes, so providing protection against inflammation [28], a result which is supported by our findings.

Recent studies have shown that the secretion of inflammatory factors, such as pro-inflammatory cytokines, are critical mediators of altered metabolism and increased ECM catabolism [3,29]. Analysis of our *in-vitro* OA model using qPCR showed that, compared to non-inflamed chondrocytes, TNF-inflamed chondrocytes increased expression of IL-6 and iNOS. These results are in keeping with other work which has also shown increased expression of iNOS after TNF inflammation [30,31] and our microarray results showed upregulation of several genes included this encoding for IL-6 (+136.82-fold), a multifunctional cytokine which is thought to contribute to the inflammatory processes in OA by promoting the production of other pro-inflammatory cytokines such as MMPs and stimulating

 doi:10.20944/preprints202409.1449.v

degradation of collagen leading to cartilage erosion and joint damage [32]. TNF increases MMP production; it also increases levels of either ADAMTS 4 or 5, and sometimes both [33–35] activating proteolytic cartilage degradation. ELISA was used to examine the expression of 3 particular MMPs: MMP-1, 2, and 13 and ADAMTS-5. As expected then, our findings showed TNF-inflamed chondrocytes expressed more MMP-13 than non-inflamed chondrocytes. Our results also showed that treatment with CM can modulate the expression of these factors, as has been seen in other works [27,36]. Microarray results also showed the upregulation of metallopeptidase inhibitor (TIMP2 and TIMP4) in samples of chondrocytes inflamed and secretome treated [37]. This is an important result as MMP-13 mediates the direct degradation of ECM components and the activation of other MMPs [25,38,39]. In the case of ADMTS-5 similar behavior was observed with levels increasing for TNF-inflamed chondrocytes and some reduction with secretome treatment. Levels of MMP-2 however, seemed largely unaffected either by TNF-inflammation or the presence of secretome. The difference in behavior between MMP-2 tested may be related to the substrate specificity of MMPs which in turn could explain the many different damage and cell-dependent inflammatory phenotypes [11]. The cytokine TNF has been shown to upregulate MMPs production in chondrocytes through various pathways including via the activation of: mitogen-activated protein kinase (MAPK), NF-kB, or activator protein 1 (AP-1) [11,24]. Considering NF-κB in particular, when this transcription factor activated in response TNF it is translocated into the cell nucleus where it binds to specific DNA sequences triggering gene transcription. In chondrocytes this process is known play a key role in TNF-induced expression of MMPs, ADAMTSs and, indeed, inflammatory cytokines themselves [34]. The key role of NF-κB and how TNF regulates these inflammatory and catabolic mediators makes it of particular interest to the understanding of OA [40] and thus, we chose to examine the influence of secretome on NF-κB activation. Our results show that secretome significantly reduces nuclear translocation in TNF-inflamed chondrocytes. This suggests that observed reductions in the expression of certain catabolic and pro-inflammatory molecules following treatment with secretome, may be due to secretome's ability to inhibit NF-*κ*B translocation.

Based on the microarray analysis and considering the TNF-inflamed/non-inflamed chondrocyte comparison (Table 1) of particular interest was the upregulation of the gene that encodes for CCL-5 and CCL2 respectively in the TNF-inflamed/non-inflamed chondrocyte comparison, in second comparison treated with secretome, it was the most downregulated. This demonstrates that the secretome is able to modulate the expression of these genes, supporting the findings of previous work [27,28,41].

As OA progresses chondrocytes lose their differentiated phenotype and begin to behave like the terminally differentiated (hypertrophy-like) chondrocytes seen in bone growth plates. Indeed, it has been shown that various hypertrophy markers, including RUNX-2 and ColX are seen at elevated levels both in *in vitro* models of OA and among individuals with OA [26,42]. The (master) transcription factor for the formation of cartilage is Sox-9 [5,43]. This factor upregulates early chondrogenic genes such Col2a1, Col11a2, and ACAN; it also enhances the differentiation of mesenchymal cells into chondrocytes and negatively regulates late stage endochondral ossification [43,44]. Conversely RUNX2, a transcription regulator for type X collagen and established marker for chondrocyte hypertrophy is involved in the calcification and degradation of cartilage matrices and directly implicated in the pathogenesis of osteoarthritis [42,45,46]. Our results indicate that secretome significantly inhibited RUNX2 expression which in turn promoted Sox-9 upregulation [47]. The inhibition of RUNX2 may also be responsible for the observed increases in Col2a1 and ACAN expression seen in our data.

Two key targets of cartilage degeneration during OA are Col2a1 and the proteoglycan ACAN, the former being degraded by the collagenase MMP13, ADAMTS 4 and 5 [24,34,35]. In agreement with the results of other work of Platas et al. [48], the present study shows clear evidence that the treatment of inflamed chondrocytes with secretome upregulates the expression of both cartilage ECM genes: Col2A1 and ACAN. Indeed, the expression of Col2a1 and ACAN in samples treated with secretome was greater than that seen in either TNF-inflamed samples or non-inflamed samples. These findings suggest that secretome could provide protection against OA. In addition, microarray results

 doi:10.20944/preprints202409.1449.v

showed an upregulation in genes as versican, a protein involved in cell adhesion, proliferation, migration, and angiogenesis; it also plays a central role in morphogenesis and tissue maintenance [49].

4. Materials and Methods

4.1. Biological Material

The primary cells used in the experimental procedures described here were all sourced from Innoprot® (Pamplona, Spain): Human adipose-derived mesenchymal stem cells (HAdMSC, Ref. P10763) and human chondrocytes (HC, Ref. P10970). Cells are cryopreserved at passage one and delivered frozen.

4.1.1. ASC and Chondrocyte Cultivation

Cells were resuspended and proliferated (~ 1 x 106 cells) in T150 flasks with DMEMc (DMEM, Hyclone®, Washington, USA) supplemented with 10% (v/v) fetal bovine serum (FBS, Hyclone®) and 1% (v/v) penicillin/streptomycin (Hyclone®) at 37°C in a humid atmosphere containing 5% CO_2.

4.2. Secretome or Conditioned Medium (CM) Collection

ASCs expanded over two passages (~ 1 x 106 cells) were maintained in DMEMc (DMEM supplemented with 10% (v/v) FBS and 1% (v/v) penicillin/streptomycin) at 37°C in a humid atmosphere containing 5% CO_2 to approximately 80% confluency. To avoid possible contamination from factors present in the FBS, cell culture supernatants (CM) were collected 24 h after the cells were supplemented with a mix of serum-free DMEM with 1% penicillin/streptomycin. Secretome protein concentration was measured using a Micro BCA Protein Assay Kit®, using BSA as a standard following the manufacturer's instructions. Protein concentration in CM was 50 μg/mL.

4.3. In-Vitro Model of Chondrocyte Inflammation

Chondrocytes (P2) were cultured in a 6-well plate (~ 1 x 105 cells). When 80% cellular confluence was reached samples were treated as follows:

- Group 1 (non-inflamed chondrocytes): chondrocytes cultured in a mix of serum-free DMEM and 1% penicillin/streptomycin.
- Group 2 (ASC control samples): ASCs cultured in a mix of serum-free DMEM and 1% penicillin/streptomycin.
- Group 3 (TNF-inflamed chondrocytes): chondrocytes cultured in a mix of serum-free DMEM and 1% penicillin/streptomycin plus TNF (25 ng/mL).
- Group 4 (CM-treated TNF-inflamed chondrocytes): chondrocytes were treated with TNF (25 ng/mL) and conditioned medium-CM (50 μg/mL).

After 12 hours further incubation, cell samples were collected and analyzed using different assays.

4.4. Gene Expression Analysis

4.4.1. Quantitative Real-Time PCR (qPCR)

Total RNA extraction from cell cultures was performed using the GeneMATRIX universal RNA purification kit (EURx®, Poland) following the manufacturer's instructions. RNA concentration was determined using NanoDrop® ND-1000 UV-Vis spectrophotometer (Thermo Scientific®, Massachusetts, USA). A high-capacity cDNA reverse transcription kit (Applied Biosystems®, Massachusetts, USA) was used to synthesize cDNA from 1000 ng of total RNA, following the manufacturer's instructions. Primers were designed with the OLIGO7® primer design tool and are listed in Table 2 and ACT-β was used as a control for the input RNA level. The qPCR reactions were performed using Power SYBR™ Green PCR Master Mix 2× (Applied Biosystems®) in a total volume

 doi:10.20944/preprints202409.1449.v

of 20 µl and on a StepOne real-time PCR system (Applied Biosystems®). Target gene expression was calculated by the 2–ΔΔCt method and normalized to the control gene, ACT-β.

Table 2. Primer sequences and conditions used for qPCR.

Gen	NCBI RefSeq	Forward/Reverse (5′-3′)	Tª melting ºC	Product size (bp)
ACT-β	NM_001101.3	CCCTCCATCGTCCACCGCAAATGCT CTGCTGTCACCTTCACCGTTCCAGT	59.7 58.0	131
IL-6	NM_000600.3	ATAACCACCCCTGACCCAA CCATGCTACATTTGCCGAA	74.4 72.5	169
iNOS	NM_000625.4	AACGTTGCTCCCCATCAAGCCCTT AGCAGCAAGTTCCATCTTTCACCCACT	54.2 54.1	130
MMP-13	NM_002427.3	CCAGAACTTCCCAACCGTATTGATGC TGCCTGTATCCTCAAAGTGAACAGC	72.3 69.1	145
TNF	NM_000594.3	CCTGAAAACAACCCTCAGACGCCACA TCCTCGGCCAGCTCCACGTCCC	77.9 79.3	155
RUNX2	NM_001024630.3	AAGCTTGATGACTCTAAACC TCTGTAATCTGACTCTGTCC	55.1 54.0	164
COLX	NM_000006.12	GCTAGTATCCTTGAACTTGG CCTTTACTCTTTATGGTGTAGG	55.5 56.1	129
Sox-9	NM_000346.4	AGTTTTGGGGGTTAACTTTG AAGCTTACCAAATGCTTCTC	59.4 57.7	132
ACAN	NM_001369268.1	CTGCCCAACTACCCGGCCAT TGCGCCCTGTCAAAGTCGAG	72.1 71.0	200
Col2a1	NM_001844.5	CCCATCTGCCCAACTGACC CACCTTTGTCACCACGATCCC	58.5 58.2	166

4.4.2. Microarray

A microarray was performed to assess the expression levels of whole transcriptome. The samples used were as described in section 3. RNA integrity, size, and quantification were assessed using RNA Nano Chips with a Bioanalyser (Agilent Technologies®, California, USA) and a Qubit® 2.0

 doi:10.20944/preprints202409.1449.v

Fluorometer (Life Technologies®, California, USA), respectively. Whole genome expression characterization was performed using a Human HT12 v4 BeadChip (Illumina Inc®, California, USA). Synthesis of cRNA was performed with the TargetAmp® Nano-g® Biotin-aRNA labeling kit for the Illumina®, Epicentre system (catalogue number TAN07924) and subsequent amplification, tagging, and hybridization were performed according to the Whole-Genome Gene Expression Direct Hybridization Illumina Inc® protocol. Raw data were extracted using GenomeStudio analysis software (Illumina Inc®). Subsequently, data were processed and analyzed in the R statistical computing environment using the R packages designed by the Bioconductor project [18,19]. Using the lumi package [18,20], raw expression data were background corrected, log2 transformed and quartile normalized.

Pairwise comparisons of gene expression were performed for each of the sample groups. Data were fitted to a linear model and empirical Bayes moderated t-statistics were calculated using the limma package [18]. P-values were adjusted by determining false discovery rates (FDR) using the Benjamini-Hochberg procedure [21]. A gene was considered differentially expressed if at least one of its associated probes had an FDR-adjusted p-value less than 0.05 and an absolute fold change greater than 2. Differentially expressed genes (DEGs) were loaded into the Panther Gene Ontology database and their cellular components, molecular functions and biological processes were analyzed using the database's online gene function annotation tools [22].

4.5. Nuclear Factor Kappa B (NF-κB) Activity Assay

Chondrocytes were seeded in two Nunc Lab-Tek Chamber Slide Systems (Thermo Fisher Scientific®) (3×105 cells per well). TNF (25 ng/mL) and/or CM (50 µg/mL) depending on the sample type (see section 3) were then added and samples were incubated for 12 hours. After this period, cells were fixed using 2% formaldehyde in PBS for 15 minutes at room temperature before being treated overnight at 4°C with human antip65-NFB pS529-FITC antibody (Miltenyi Biotech®, Radolfzell, Germany). Finally, chamber slides were mounted using Vectashield mounting medium containing DAPI for inspection under a confocal microscope (Zeiss®, Jena, Germany). NIH Image J Software® was used to analyze the fluorescence images of cell nuclei obtained to estimate the total number of positive translocated cells in each sample.

4.6. Enzyme-Linked Immunosorbent Assay (ELISA)

After 12h of stimulation with TNF (25ng/mL) chondrocyte samples were tested for concentrations of MMP-1, MMP-2 and MMP-13, and ADAMTS-5 using a specific human MMP-1 (Elabscience®, Texas, USA), MMP-2 (Elabscience®), MMP-13 (Ray Bio®, GA, USA) and ADAMST-5 (Elabscience®) ELISA kit, following the manufacturer's protocols. Measurements were carried out at 450 nm using a Multiskan GO multi-plate spectrophotometry (Thermo Fisher Scientific®) and concentrations were calculated by comparing them to known standards.

4.7. Protein Analysis

4.7.1. Total Protein Extraction and Quantification

Chondrocytes plated in 6 well-culture dishes were scraped in 200 µl of RIPA lysis buffer [500 mL stock solution: 1.6 mM NaH2PO4 (Merck®, Darmstadt, Germany), 8.4 mM Na2HPO4 (Merck®), 0.1 % TritonX-100 (VWR®), 0.1 M NaCl (Ambion®, Massachusetts, USA), 0.1 % sodium dodecyl sulphate (SDS; Thermo Fisher Scientific®) and ddH2O] supplemented with sodium deoxycholate (Merck®), 1 mM sodium fluoride and 1X protease and phosphatase inhibitor cocktails (Roche®, Basilea, Switzerland). Protein concentration was quantified using the Bicinchoninic acid (BCA) protein assay (Bio-Rad®, California, USA) in a SpectraMax microplate reader (bioNova Scientific®, Madrid, Spain).

 doi:10.20944/preprints202409.1449.v

4.7.2. Western Blotting Analysis

Samples containing 5 μg total protein were combined with 5X loading buffer [250 mM Tris-HCl (Merck®) pH 6.8, 500 mM β-mercaptoethanol (Merck®), 50 % glycerol (Merck®), 10 % SDS (Merck®), and bromophenol blue (Merck®)] in H2O and denatured by boiling. Proteins were resolved by SDS-PAGE in 8 %, 11 % or 15 % acrylamide gels, using Mini-PROTEAN Electrophoresis System (Bio-Rad®). Fractionated proteins were transferred onto nitrocellulose membranes by electroblotting using a Mini Trans-Blot cell (Bio-Rad®). Membranes were blocked with 5 % nonfat dry milk in 1X Tris Buffer Saline (TBS) [50 mM Tris, 150 mM NaCl (Merck®), pH 8.0) containing 0.1 % Tween-20 (Merck®) (TBST-0.1 %)] and incubated with primary antibodies overnight at 4ºC (Table 3). Horseradish peroxidase-conjugated antibodies were used as secondary antibodies to detect immunoreactive protein bands by Western Lightning Enhanced Chemiluminiscence (ECL) Reagent (PerkinElmer®) with X-ray imaging [(Fujifilm®) in a Curix 60 Developer (Agfa®)].

Table 3. Primary antibodies used for protein detection. Target proteins of the antibodies used dilution and company are specified.

Target protein	Dilution	Company
β-Actin	1:5,000	Merck®
Sox-9	1:1,000	Cell Signaling®
RUNX2	1:1,000	Cell Signaling®
Col2a1	1:1,000	Cell Signaling®
COLX	1:1,000	Santa Cruz Biotechnology®
ACAN	1:1,000	Cell Signaling®

4.7.3. Confocal Microscopy

Cells were sub-cultured on 8-well Nunc Lab-Tek chamber slide system (Thermo Fisher Scientific®) (2×103 cells/well). Cells were fixed with 2% paraformaldehyde for 15 minutes prior to overnight incubation with primary mouse anti-COLX (Santa Cruz Technologies®, Texas, USA), anti-Col2a1, anti-ACAN, anti-Sox-9 and anti-RUNX2 antibodies (Cell Signaling®, Massachusetts, USA) (1:100) at 4°C, after which they were treated with secondary biotinylated anti-mouse antibodies (1:100) (Abcam®, Cambridge, UK). Cells were then stained with streptavidin-Alexa 488 and streptavidin-Alexa 568 antibodies (1:100) (Invitrogen®, Massachusetts, USA). Finally, chamber slides were mounted using Vectashield mounting medium (Vector Laboratories®, USA) containing DAPI. After staining, cells were imaged with a confocal microscope (Zeiss®).

 doi:10.20944/preprints202409.1449.v

4.8. Statistical Analysis

All experiments were completed in triplicate and results expressed as the mean ± SD of the three experimental outcomes. Statistical analysis was performed using IBM® SPSS® Statistics (IBM Corp., Armonk, NY, USA). Significant differences among groups were determined using ANOVA followed by post-hoc analysis for multiple group comparisons or Student's t-test for two group comparisons. Results with $p<0.05$ were considered statistically significant.

5. Conclusions

Our results suggest secretome possesses several properties of potential benefit in the treatment of OA including anti-inflammatory properties, the ability to stimulate proteoglycan production, and inhibit chondrocyte catabolism and the production of certain proteolytic enzymes such metalloproteases and inflammatory mediators such as TNF, IL-6 or iNOS. In addition, secretome appears to have a protective effect for cartilage revealed by its ability to inhibit or decrease levels of hypertrophy markers such as RUNX2, COLX and MMP-13; increase production of ECM component genes Col2a1 and ACAN production; and upregulate expression of the chondrogenic marker Sox-9. In this way, secretome represents a potentially effective treatment for OA.

Author Contributions: VV: EG & MG concepted and designed the study. VV acquired data and drafted the article. ME, SP & EP performed the experiments. JA, AA & NN performed microarray analysis and interpretation of RNA data. EG performed the analysis of immune assays. All authors revised the manuscript critically for important intellectual content and approved the final version to be submitted. VV and EG take responsibility for the integrity of the work as a whole, from inception to finished article.

Funding: "This research was funded by MCIN/AEI/10.13039/501100011033 (CEX2021-001136-S) and the Regional Government of Castile and León (Spain) for financial support.

Institutional Review Board Statement: Not applicable.

Informed Consent Statement: Not applicable.

Data Availability Statement: The data used to support the findings of this study are available from the corresponding author upon request. All the microarray data are deposited in the public functional genomics data repository Gene Expression Omnibus (GEO) supporting MIAME-compliant data submissions. To review GEO accession GSE239343: Go to https://www.ncbi.nlm.nih.gov/geo/query/acc.cgi?acc=GSE239343 Enter token ivevkgmkvfyvler into the box.

Acknowledgments: We thank Mª Elisa López González and Cintia Miranda Rodríguez for their technical support.

Conflicts of Interest: The authors declare no conflicts of interest.

References

1. Cui, A.; Li, H.; Wang, D.; Zhong, J.; Chen, Y.; Lu, H. Global, Regional Prevalence, Incidence and Risk Factors of Knee Osteoarthritis in Population-Based Studies. EClinicalMedicine 2020, 29–30, 100587, doi:10.1016/j.eclinm.2020.100587.
2. Funck-Brentano, T.; Cohen-Solal, M. Subchondral Bone and Osteoarthritis. Curr. Opin. Rheumatol. 2015, 27, 420–426, doi:10.1097/BOR.0000000000000181.
3. Fernandes, J.C.; Martel-Pelletier, J.; Pelletier, J.-P. The Role of Cytokines in Osteoarthritis Pathophysiology. Biorheology 2002, 39, 237–246.
4. Tetlow, L.C.; Adlam, D.J.; Woolley, D.E. Matrix Metalloproteinase and Proinflammatory Cytokine Production by Chondrocytes of Human Osteoarthritic Cartilage: Associations with Degenerative Changes. Arthritis Rheum. 2001, 44, 585–594, doi:10.1002/1529-0131(200103)44:3<585::AID-ANR107>3.0.CO;2-C.
5. Zhang, Q.; Ji, Q.; Wang, X.; Kang, L.; Fu, Y.; Yin, Y.; Li, Z.; Liu, Y.; Xu, X.; Wang, Y. SOX9 Is a Regulator of ADAMTSs-Induced Cartilage Degeneration at the Early Stage of Human Osteoarthritis. Osteoarthr. Cartil. 2015, 23, 2259–2268, doi:10.1016/j.joca.2015.06.014.

6. Mengshol, J.A.; Vincenti, M.P.; Coon, C.I.; Barchowsky, A.; Brinckerhoff, C.E. Interleukin-1 Induction of Collagenase 3 (Matrix Metalloproteinase 13) Gene Expression in Chondrocytes Requires P38, c-Jun N-Terminal Kinase, and Nuclear Factor KB: Differential Regulation of Collagenase 1 and Collagenase 3. Arthritis Rheum. 2000, 43, 801, doi:10.1002/1529-0131(200004)43:4<801::AID-ANR10>3.0.CO;2-4.
7. Goldring, S.R.; Goldring, M.B. Bone and Cartilage in Osteoarthritis: Is What's Best for One Good or Bad for the Other? Arthritis Res. Ther. 2010, 12, 143, doi:10.1186/ar3135.
8. Phillips KL, Chiverton N, Michael AL, Cole AA, Breakwell LM, Haddock G, Bunning RA, Cross AK, L.M.C. The Cytokine and Chemokine Expression Profile of Nucleus Pulposus Cells: Implications for Degeneration and Regeneration of the Intervertebral Disc. Biomaterials 2006, 12, 73–84, doi:10.1089/ten.TEA.2011.0360.
9. Attur, M.G.; Patel, I.R.; Patel, R.N.; Abramson, S.B.; Amin, A.R. Autocrine Production of IL-1 Beta by Human Osteoarthritis-Affected Cartilage and Differential Regulation of Endogenous Nitric Oxide, IL-6, Prostaglandin E2, and IL-8. Proc. Assoc. Am. Physicians 110, 65–72.
10. Clancy, R.M.; Amin, A.R.; Abramson, S.B. The Role of Nitric Oxide in Inflammation and Immunity. Arthritis Rheum. 1998, 41, 1141–1151, doi:10.1002/1529-0131(199807)41:7<1141::AID-ART2>3.0.CO;2-S.
11. Kawasaki, Y.; Xu, Z.Z.; Wang, X.; Park, J.Y.; Zhuang, Z.Y.; Tan, P.H.; Gao, Y.J.; Roy, K.; Corfas, G.; Lo, E.H.; et al. Distinct Roles of Matrix Metalloproteases in the Early- and Late-Phase Development of Neuropathic Pain. Nat. Med. 2008, 14, 331–336, doi:10.1038/nm1723.
12. Orozco, L.; Munar, A.; Soler, R.; Alberca, M.; Soler, F.; Huguet, M.; Sentís, J.; Sánchez, A.; García-Sancho, J. Treatment of Knee Osteoarthritis With Autologous Mesenchymal Stem Cells. Transplant. J. 2013, 95, 1535–1541, doi:10.1097/TP.0b013e318291a2da.
13. Kristjánsson, B.; Honsawek, S. Current Perspectives in Mesenchymal Stem Cell Therapies for Osteoarthritis. Stem Cells Int. 2014, 2014, 1–13, doi:10.1155/2014/194318.
14. Jung, Y.; Bauer, G.; Nolta, J.A. Concise Review: Induced Pluripotent Stem Cell-Derived Mesenchymal Stem Cells: Progress toward Safe Clinical Products. Stem Cells 2012, 30, 42–47, doi:10.1002/stem.727.
15. L., P.K.; Kandoi, S.; Misra, R.; S., V.; K., R.; Verma, R.S. The Mesenchymal Stem Cell Secretome: A New Paradigm towards Cell-Free Therapeutic Mode in Regenerative Medicine. Cytokine Growth Factor Rev. 2019, 46, 1–9.
16. Lavoie, J.R.; Rosu-Myles, M. Uncovering the Secretes of Mesenchymal Stem Cells. Biochimie 2013, 95, 2212–2221.
17. Pawitan, J.A. Prospect of Stem Cell Conditioned Medium in Regenerative Medicine. Biomed Res. Int. 2014, 2014, 965849, doi:10.1155/2014/965849.
18. JM, W.; GK, S. LimmaGUI: A Graphical User Interface for Linear Modeling of Microarray Data. Bioinformatics 2004, 20, 3705–3706, doi:10.1093/BIOINFORMATICS/BTH449.
19. RC, G.; VJ, C.; DM, B.; B, B.; M, D.; S, D.; B, E.; L, G.; Y, G.; J, G.; et al. Bioconductor: Open Software Development for Computational Biology and Bioinformatics. Genome Biol. 2004, 5, doi:10.1186/GB-2004-5-10-R80.
20. P, D.; WA, K.; SM, L. Lumi: A Pipeline for Processing Illumina Microarray. Bioinformatics 2008, 24, 1547–1548, doi:10.1093/BIOINFORMATICS/BTN224.
21. Benjamini, Y.; Hochberg, Y. Controlling the False Discovery Rate: A Practical and Powerful Approach to Multiple Testing. J. R. Stat. Soc. Ser. B 1995, 57, 289–300, doi:10.1111/J.2517-6161.1995.TB02031.X.
22. M, A.; CA, B.; JA, B.; D, B.; H, B.; JM, C.; AP, D.; K, D.; SS, D.; JT, E.; et al. Gene Ontology: Tool for the Unification of Biology. The Gene Ontology Consortium. Nat. Genet. 2000, 25, 25–29, doi:10.1038/75556.
23. Zhang, Y.; Liu, D.; Tadum, D.; Vithran, A.; Kwabena, B.R. CC Chemokines and Receptors in Osteoarthritis : New Insights and Potential Targets. Arthritis Res. Ther. 2023, 1–11, doi:10.1186/s13075-023-03096-6.
24. Wang, M.; Sampson, E.R.; Jin, H.; Li, J.; Ke, Q.H.; Im, H.-J.; Chen, D. MMP13 Is a Critical Target Gene during the Progression of Osteoarthritis. Arthritis Res. Ther. 2013, 15, R5, doi:10.1186/ar4133.
25. Davidson, R.K.; Waters, J.G.; Kevorkian, L.; Darrah, C.; Cooper, A.; Donell, S.T.; Clark, I.M. Expression Profiling of Metalloproteinases and Their Inhibitors in Synovium and Cartilage. Arthritis Res. Ther. 2006, 8, 1–10, doi:10.1186/ar2013.
26. Zhong, L.; Huang, X.; Karperien, M.; Post, J.N. The Regulatory Role of Signaling Crosstalk in Hypertrophy of MSCs and Human Articular Chondrocytes. Int. J. Mol. Sci. 2015, 16, 19225–19247, doi:10.3390/ijms160819225.

27. D'arrigo, D.; Roffi, A.; Cucchiarini, M.; Moretti, M.; Candrian, C.; Filardo, G. Secretome and Extracellular Vesicles as New Biological Therapies for Knee Osteoarthritis: A Systematic Review. J. Clin. Med. 2019, 8, doi:10.3390/JCM8111867.
28. Zhang, Y.; Liang, X.; Liao, S.; Wang, W.; Wang, J.; Li, X.; Ding, Y.; Liang, Y.; Gao, F.; Yang, M.; et al. Potent Paracrine Effects of Human Induced Pluripotent Stem Cell-Derived Mesenchymal Stem Cells Attenuate Doxorubicin-Induced Cardiomyopathy. Sci. Rep. 2015, 5, 11235, doi:10.1038/srep11235.
29. Wojdasiewicz, P.; Poniatowski, Ł.A.; Szukiewicz, D. The Role of Inflammatory and Anti-Inflammatory Cytokines in the Pathogenesis of Osteoarthritis. Mediators Inflamm. 2014, 2014, 1–19, doi:10.1155/2014/561459.
30. Yang, Y.; Gao, S.-G.; Zhang, F.-J.; Luo, W.; Xue, J.-X.; Lei, G.-H. Effects of Osteopontin on the Expression of IL-6 and IL-8 Inflammatory Factors in Human Knee Osteoarthritis Chondrocytes. Eur. Rev. Med. Pharmacol. Sci. 2014, 18, 3580–3586.
31. Porée, B.; Kypriotou, M.; Chadjichristos, C.; Beauchef, G.; Renard, E.; Legendre, F.; Melin, M.; Gueret, S.; Hartmann, D.J.; Malléin-Gerin, F.; et al. Interleukin-6 (IL-6) and/or Soluble IL-6 Receptor down-Regulation of Human Type II Collagen Gene Expression in Articular Chondrocytes Requires a Decrease of Sp1.Sp3 Ratio and of the Binding Activity of Both Factors to the COL2A1 Promoter. J. Biol. Chem. 2008, 283, 4850–4865, doi:10.1074/JBC.M706387200.
32. Scheller, J.; Chalaris, A.; Schmidt-Arras, D.; Rose-John, S. The Pro- and Anti-Inflammatory Properties of the Cytokine Interleukin-6; 2011; Vol. 1813, pp. 878–888;.
33. Gabay, C.; Lamacchia, C.; Palmer, G. IL-1 Pathways in Inflammation and Human Diseases. Nat. Rev. Rheumatol. 2010, 6, 232–241, doi:10.1038/nrrheum.2010.4.
34. Rogerson, F.M.; Chung, Y.M.; Deutscher, M.E.; Last, K.; Fosang, A.J. Cytokine-Induced Increases in ADAMTS-4 Messenger RNA Expression Do Not Lead to Increased Aggrecanase Activity in ADAMTS-5-Deficient Mice. Arthritis Rheum. 2010, 62, 3365–3373, doi:10.1002/art.27661.
35. Carlos Rodríguez-Manzaneque, J.; Westling, J.; Thai, S.N.-M.; Luque, A.; Knauper, V.; Murphy, G.; Sandy, J.D.; Iruela-Arispe, M.L. ADAMTS1 Cleaves Aggrecan at Multiple Sites and Is Differentially Inhibited by Metalloproteinase Inhibitors. Biochem. Biophys. Res. Commun. 2002, 293, 501–508, doi:10.1016/S0006-291X(02)00254-1.
36. Camassola, M.; de Macedo Braga, L.M.G.; Chagastelles, P.C.; Nardi, N.B. Methodology, Biology and Clinical Applications of Human Mesenchymal Stem Cells. In Methods in molecular biology (Clifton, N.J.); 2012; Vol. 879, pp. 491–504.
37. Lozito, T.P.; Jackson, W.M.; Nesti, L.J.; Tuan, R.S. Human Mesenchymal Stem Cells Generate a Distinct Pericellular Zone of MMP Activities via Binding of MMPs and Secretion of High Levels of TIMPs. Matrix Biol. 2014, 34, 132–143, doi:10.1016/j.matbio.2013.10.003.
38. Cawston, T. Matrix Metalloproteinases and TIMPs: Properties and Implications for the Rheumatic Diseases. Mol. Med. Today 1998, 4, 130–137, doi:10.1016/S1357-4310(97)01192-1.
39. Cawston, T.E.; Wilson, A.J. Understanding the Role of Tissue Degrading Enzymes and Their Inhibitors in Development and Disease. Best Pract. Res. Clin. Rheumatol. 2006, 20, 983–1002, doi:10.1016/j.berh.2006.06.007.
40. Rigoglou, S.; Papavassiliou, A.G. The NF-KB Signalling Pathway in Osteoarthritis. Int. J. Biochem. Cell Biol. 2013, 45, 2580–2584, doi:10.1016/j.biocel.2013.08.018.
41. Sun, Y.; Liu, G.; Zhang, K.; Cao, Q.; Liu, T.; Li, J. Mesenchymal Stem Cells-Derived Exosomes for Drug Delivery. Stem Cell Res. Ther. 2021 121 2021, 12, 1–15, doi:10.1186/S13287-021-02629-7.
42. Bruderer, M.; Richards, R.G.; Alini, M.; Stoddart, M.J. Role and Regulation of Runx2 in Osteogenesis. Eur. Cells Mater. 2014, 28, 269–286, doi:10.22203/eCM.v028a19.
43. Haag, J.; Gebhard, P.M.; Aigner, T. SOX Gene Expression in Human Osteoarthritic Cartilage. Pathobiology 2008, 75, 195–199, doi:10.1159/000124980.
44. Mariani, E.; Pulsatelli, L.; Facchini, A. Signaling Pathways in Cartilage Repair. Int. J. Mol. Sci. 2014, 15, 8667–8698, doi:10.3390/ijms15058667.
45. Nishimura, R.; Hata, K.; Takahata, Y.; Murakami, T.; Nakamura, E.; Yagi, H. Regulation of Cartilage Development and Diseases by Transcription Factors. J. bone Metab. 2017, 24, 147, doi:10.11005/JBM.2017.24.3.147.

46. Zhong, L.; Huang, X.; Karperien, M.; Post, J.N.; Malemud, C.J.; Mobasheri, A. The Regulatory Role of Signaling Crosstalk in Hypertrophy of MSCs and Human Articular Chondrocytes. OPEN ACCESS Int. J. Mol. Sci 2015, 16, 19226, doi:10.3390/ijms160819225.
47. Niada, S.; Giannasi, C.; Gomarasca, M.; Stanco, D.; Casati, S.; Brini, A.T. Adipose-Derived Stromal Cell Secretome Reduces TNFα-Induced Hypertrophy and Catabolic Markers in Primary Human Articular Chondrocytes. Stem Cell Res. 2019, 38, 101463, doi:10.1016/j.scr.2019.101463.
48. Platas, J.; Guillén, M.I.; Del Caz, M.D.P.; Gomar, F.; Mirabet, V.; Alcaraz, M.J. Conditioned Media from Adipose-Tissue-Derived Mesenchymal Stem Cells Downregulate Degradative Mediators Induced by Interleukin-1 β in Osteoarthritic Chondrocytes. Mediators Inflamm. 2013, 2013, doi:10.1155/2013/357014.
49. Casagrande, D.; Stains, J.P.; Murthi, A.M. Identification of Shoulder Osteoarthritis Biomarkers: Comparison between Shoulders with and without Osteoarthritis. J. shoulder Elb. Surg. 2015, 24, 382–390, doi:10.1016/J.JSE.2014.11.039.